PHYSICAL REVIEW E VOLUME 51, NUMBER 5 MAY 1995

Heat flux vector in highly inhomogeneous nonequilibrium fluids

B. D. Todd, Peter J. Daivis, and Denis J. Evans
Research School of Chemistry, Australian National University, Canberra, Australian Capital Territory 0200, Australia

(Received 12 December 1994)

We develop a simple, efficient, and general statistical mechanical technique, based upon the previously developed method of planes (MOP) technique of calculating the pressure tensor, in order to calculate the heat flux vector of an atomic fluid. The method is applied to the case of Poiseuille flow through a narrow channel and is compared to the corresponding Irving-Kirkwood heat flux vector, using the first approximation (IK1). Our exact MOP method is shown to be more efficient than the approximate IK1 approach. Additionally, for the special case of planar Poiseuille flow, we derive an alternative mesoscopic expression by integrating the energy continuity equation. This mesoscopic calculation is shown to be extremely efficient and is in excellent numerical agreement with the MOP.

PACS number(s): 03.40.Gc, 02.50.−r, 51.10.+y, 05.70.Ln

I. INTRODUCTION

The heat flux vector of a statistical ensemble of fluid atoms is usually calculated by the application of the Irving-Kirkwood statistical mechanical theory of transport processes [1,2]. Once the heat flux vector is known the thermal conductivity of the fluid may be calculated by either the Green-Kubo or the NEMD technique [2,3].

The Irving-Kirkwood technique leads to the following expression for the ensemble averaged value of the heat flux vector:

$$\mathbf{J}_q(\mathbf{r},t)=\frac{1}{V}\left\langle\sum_i [\mathbf{v}_i(t)-\mathbf{u}(\mathbf{r},t)]U_i(t)-\tfrac{1}{2}\sum_{i,j}\mathbf{r}_{ij}(t)[\mathbf{v}_i(t)-\mathbf{u}(\mathbf{r},t)]\cdot\mathbf{F}_{ij}(t)O_{ij}(t)\middle|\mathbf{r}_i(t)=\mathbf{r}\right\rangle , \tag{1}$$

where V is the volume of the system, $\mathbf{v}_i$ is the laboratory velocity of particle i, $\mathbf{u}$ is the streaming velocity of the fluid, U_i is the contribution of particle i to the internal energy of the fluid, $\mathbf{r}_{ij}$ is defined here as $\mathbf{r}_j-\mathbf{r}_i$, and $\mathbf{F}_{ij}$ is the intermolecular force on atom i due to atom j. O_{ij} is defined as

$$O_{ij}=1-\frac{1}{2!}\mathbf{r}_{ij}\cdot\frac{\partial}{\partial\mathbf{r}}+\cdots+\frac{1}{n!}\left[-\mathbf{r}_{ij}\cdot\frac{\partial}{\partial\mathbf{r}}\right]^{n-1}+\cdots . \tag{2}$$

The $\mathbf{k}$-space version of Eq. (1) is somewhat more complicated than the corresponding $\mathbf{k}$-space expression for the pressure tensor because the streaming velocity is a function of $\mathbf{r}$. It is probably for this reason that it has apparently never appeared in the literature. Therefore, we include a discussion of the Fourier transform of the heat flux vector in a fluid with an arbitrary $\mathbf{r}$-dependent streaming velocity, preceded by a more direct derivation of the Irving-Kirkwood heat flux vector, in the Appendix.

If the fluid is uniform in space, $O_{ij}=1$ and Eq. (1) is an accurate and computationally simple expression to use. However, previous work [4] has shown that for systems in which the fluid density is not homogeneous in space, such as the case of flow through narrow channels or pores, the higher-order O_{ij} terms cannot be ignored and the resulting expression for the heat flux vector becomes significantly more complex to compute. In what follows, the $O_{ij}=1$ approximation to Eq. (1) will be called the IK1 expression for the Irving-Kirkwood heat flux vector.

This paper was thus motivated by the desire to develop a simple technique that could accurately calculate the heat flux vector for a system in which the density is not spatially homogeneous. We apply our general technique to the specific case of planar Poiseuille flow through a narrow channel.

II. THEORY

A. Method of planes expression for the heat flux vector

The technique we develop here is based upon the method of planes (MOP) derivation we used previously to calculate the pressure tensor of an atomic liquid [4] and involves calculating the heat flux through any number of planes located anywhere in the system whose normals are parallel to, say, the y axis. It is assumed that the properties of the system are homogeneous in the two directions parallel to the planes. This would be the case, for example, with planar Poiseuille flow, in which a pressure head in the x direction drives the fluid into nonequilibrium steady state and in which heat will only flow in the y direction.

We begin by writing down the continuity equation for the local energy density of the fluid [2,5]

1063-651X/95/51(5)/4362(7)/$06.00

$$\frac{\partial}{\partial t}[\rho(\mathbf{r},t)e(\mathbf{r},t)] = -\nabla\cdot[\mathbf{J}_q(\mathbf{r},t)+\rho(\mathbf{r},t)e(\mathbf{r},t)\mathbf{u}(\mathbf{r},t)+\mathbf{P}(\mathbf{r},t)\cdot\mathbf{u}(\mathbf{r},t)] \ . \tag{3}$$

In **k** space, this becomes

$$\frac{\partial}{\partial t}\rho e(\mathbf{k},t)=i\mathbf{k}\cdot[\mathbf{J}_q(\mathbf{k},t)+\mathcal{F}\{\rho e\mathbf{u}\}+\mathcal{F}\{\mathbf{P}\cdot\mathbf{u}\}] \ , \tag{4}$$

where $\mathbf{J}_q(\mathbf{k},t)$ is the heat flux vector in **k** space, **P** is the pressure tensor, **u** is the streaming velocity, and $\mathcal{F}\{\ \}$ denotes a Fourier transform. Note that $\rho e(\mathbf{k},t)$ is the Fourier transform of the local energy density, defined as

$$\rho e(\mathbf{r},t)\equiv\sum_i e_i\delta(\mathbf{r}-\mathbf{r}_i) \ , \tag{5}$$

where the total energy of atom i is given by

$$e_i=\frac{\mathbf{p}_i^2}{2m}+\frac{1}{2}\sum_j \phi_{ij} \tag{6}$$

and $\mathbf{p}_i$ is the laboratory momentum of particle i.

From the microscopic expression for the energy density and the sifting property of the δ function, we find that the convection term in the Fourier transformed energy density continuity equation can be written as

$$\rho e\mathbf{u}(\mathbf{k},t)=\sum_i e_i\mathbf{u}(\mathbf{r}_i,t)e^{i\mathbf{k}\cdot\mathbf{r}_i} \ . \tag{7}$$

The time derivative of the Fourier transform of the local energy density is

$$\frac{\partial}{\partial t}\rho e(\mathbf{k},t)=i\mathbf{k}\cdot\sum_i \mathbf{v}_i e_i e^{i\mathbf{k}\cdot\mathbf{r}_i} +\frac{1}{2}\sum_i\sum_j \mathbf{v}_i\cdot\mathbf{F}_{ij}(e^{i\mathbf{k}\cdot\mathbf{r}_i}-e^{i\mathbf{k}\cdot\mathbf{r}_j}) \ . \tag{8}$$

If we now substitute (7) and (8) into the continuity equation, isolate the heat flux vector, and take the zero wave vector limit for the x and the z components of **k** (equivalent to averaging over the xz plane), we obtain

$$\begin{aligned}Aik_yJ_{qy}(k_y,t)={}&ik_y\sum_i(v_{yi}-u_{yi})e_ie^{iky_i}\\&+\tfrac{1}{2}\sum_i\sum_j\mathbf{v}_i\cdot\mathbf{F}_{ij}(e^{iky_i}-e^{iky_j})\\&-Aik_y(\mathcal{F}\{\mathbf{P}\cdot\mathbf{u}\})_y \ ,\end{aligned} \tag{9}$$

where A is the area of the xz plane and we note that $\mathbf{u}=\mathbf{u}(y)$. Dividing by ik_y and inverse Fourier transforming, we then find

$$\begin{aligned}AJ_{qy}(y,t)={}&\sum_i(v_{yi}-u_y)e_i\delta(y-y_i)\\&-\tfrac{1}{4}\sum_i\sum_j\mathbf{v}_i\cdot\mathbf{F}_{ij}[\operatorname{sgn}(y-y_i)-\operatorname{sgn}(y-y_j)]\\&-A(\mathbf{P}\cdot\mathbf{u})_y \ .\end{aligned} \tag{10}$$

The microscopic expression for the $y\alpha$ element of the pressure tensor (where α is any of x,y,z) is written as the sum of two terms, the kinetic term $P^K_{\alpha y}(y,t)$ and the potential term $P^U_{\alpha y}(y,t)$ [4]:

$$\begin{aligned}AP_{y\alpha}(y,t)&=A[P^K_{y\alpha}(y,t)+P^U_{y\alpha}(y,t)]\\&=\sum_i m_i(v_{yi}-u_y)(v_{\alpha i}-u_\alpha)\delta(y-y_i)\\&\quad-\tfrac{1}{4}\sum_i\sum_j\mathbf{F}_{ij}[\operatorname{sgn}(y-y_i)-\operatorname{sgn}(y-y_j)] \ .\end{aligned} \tag{11}$$

After substituting this into (10) we obtain finally

$$J_{qy}(y,t)=J^K_{qy}(y,t)+J^U_{qy}(y,t) \ , \tag{12}$$

where the kinetic part of the heat flux vector is given as

$$J^K_{qy}(y,t)=\frac{1}{A}\sum_i(v_{yi}-u_y)U_i\delta(y-y_i) \tag{13}$$

and the potential part is given as

$$J^U_{qy}(y,t)=-\frac{1}{4A}\sum_i\sum_j[\mathbf{v}_i-\mathbf{u}(y)]\cdot\mathbf{F}_{ij}[\operatorname{sgn}(y-y_i)-\operatorname{sgn}(y-y_j)] \ . \tag{14}$$

In deriving (12) we have used the definition of the internal energy of a particle

$$U_i=\tfrac{1}{2}m[\mathbf{v}_i-\mathbf{u}(y_i)]^2+\tfrac{1}{2}\sum_j\phi_{ij} \ , \tag{15}$$

which, unlike the expression for the total energy, excludes the streaming component of the kinetic energy and we have also used the following relationships:

$$\mathbf{u}^2(\mathbf{r},t)\sum_i m_i(\mathbf{v}_i-\mathbf{u})\delta(\mathbf{r}-\mathbf{r}_i) =\mathbf{u}^2(\mathbf{r},t)[\rho\mathbf{u}(\mathbf{r},t)-\rho\mathbf{u}(\mathbf{r},t)]=0 \ . \tag{16}$$

The instantaneous value of the y component of the heat flux vector is thus the sum of kinetic and potential contributions. It is instructive to view $J^K_{qy}(y,t)$ and $J^U_{qy}(y,t)$ as representing, respectively, the kinetic and the configurational contributions to the conductive part of the instantaneous internal energy flux. Equation (13) states that at any time t, a particle with internal energy U_i will contribute to the instantaneous energy flux through the plane if it intersects the plane at $y_i=y$ and time $t_i=t$, whereas Eq. (14) states that at any time t, even though no particle may actually intersect a plane at y, the energy distribution on both sides of a plane may change, such that a "flow" of energy could be considered to have taken place across that plane.

We also make the following observation, namely, that the streaming velocity $\mathbf{u}(y)$ used in Eqs. (13) and (14) is interpreted as the streaming velocity of the fluid evaluated *at the plane* y. It is not to be confused with the particle streaming velocity $\mathbf{u}(y_i)$. Thus all velocities $\chi_i=\mathbf{v}_i-\mathbf{u}_y$ (defined here as "plane peculiar velocities") are not the usual peculiar velocities, defined by $\mathbf{c}_i=\mathbf{v}_i-\mathbf{u}(y_i)$, but rather the velocity of atom i relative to the streaming velocity at the plane. It so happens that for the kinetic contribution to the heat flux vector we find that $\mathbf{u}(y)=\mathbf{u}(y_i)$, but this is certainly not the case for the potential component of $J_{qy}(y)$. This is a subtle but potentially important point to note. In regions where the curvature in the streaming velocity profile is significant over the range of the intermolecular potential function we might expect the plane peculiar velocities to be significantly different to the peculiar velocities and using the latter values in the calculation of $J_{qy}(y)$, instead of plane peculiar velocities χ_i, may well give us the wrong results. Where the curvature in $\mathbf{u}$ is not significant it would be expected that, averaged over time, there should be little difference in the calculation of $J_{qy}(y)$ if either peculiar or plane peculiar velocities were used.

Equation (13) can be rewritten into a form that is more accessible for computer simulation. The δ function in (13) may be rewritten in terms of the sgn function such that

$$J_{qy}^{K}(y,t)=\frac{1}{2A}\sum_i (v_{yi}-u_y)U_i\frac{d}{dy}\,\mathrm{sgn}(y-y_i)\ . \tag{17}$$

Making use of the chain rule in differentiating the sgn function gives us

$$J_{qy}^{K}(y,t)=\frac{1}{2A}\sum_i U_i\frac{d}{dt}\,\mathrm{sgn}(y-y_i)\ . \tag{18}$$

If particle i crosses the plane at a set of times $\{t_{i,m};\ i=1,\ldots,N;\ m=1,2,\ldots\}$ and if we use the sign of the y component of the peculiar velocity to tell us whether the crossing is from right to left or vice versa, (18) may be written as

$$J_{qy}^{K}(y,t)=\frac{1}{A}\sum_{t,m}\sum_i U_i\delta(t-t_{i,m})\,\mathrm{sgn}[c_{yi}(t_{i,m})]\ , \tag{19}$$

and the time averaged kinetic component of the heat flux vector can be thus expressed as

$$J_{qy}^{K}(y)=\lim_{\tau\to\infty}\frac{1}{A\tau}\sum_{0<t_{i,m}<\tau}\sum_i U_i\,\mathrm{sgn}[c_{yi}(t_{i,m})]\ . \tag{20}$$

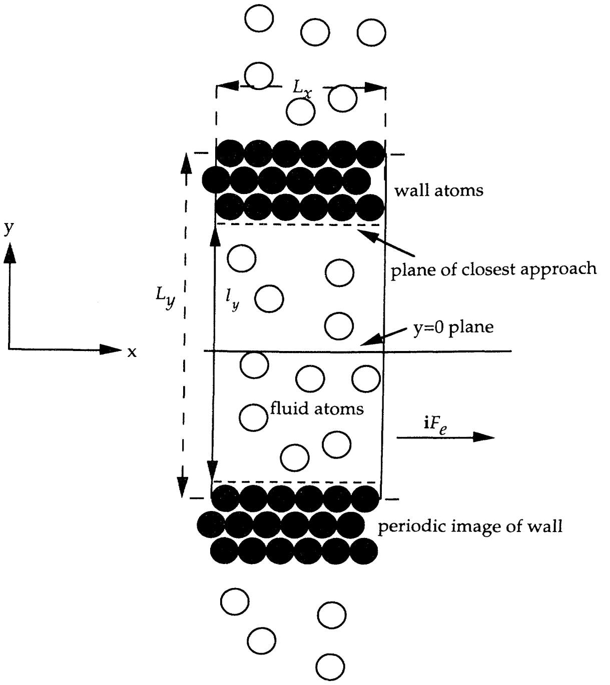

FIG. 1. Simulation geometry for planar Poiseuille flow. The z axis is normal to the page.

B. Mesoscopic derivation of the heat flux vector

There is an alternative route to calculating the heat flux vector, based on the hydrodynamical continuity equation for the specific internal energy

$$\rho\frac{dU(\mathbf{r},t)}{dt}=-\nabla\cdot\mathbf{J}_q(\mathbf{r},t)-\mathbf{P}(\mathbf{r},t)^T:\nabla\mathbf{u}(\mathbf{r},t)\ . \tag{21}$$

For a system such as ours, in which a steady-state fluid under the influence of an external field in the x direction is sandwiched between planar walls separated in the y direction (see Fig. 1), (21) reduces to

$$0=-\frac{\partial J_{qy}(y)}{\partial y}-P_{xy}(y)\gamma(y)\ , \tag{22}$$

where $\gamma(y)$ is the strain rate given by

$$\gamma(y)=\frac{\partial u_x(y)}{\partial y}$$

and $-P_{xy}(y)$ is the stress. Thus the heat flux is simply given by

$$J_{qy}(y)=-\int_0^y dy' P_{xy}(y')\gamma(y')\ . \tag{23}$$

$P_{xy}(y)$ may be calculated by either of two ways, MOP or by integrating the momentum conservation equation (the IMC method) [4]. We call this derivation mesoscopic because it does not explicitly refer to molecular quantities. We refer to (23) as the IEC method for determining the heat flux.

III. SIMULATION DETAILS

A. Equations of motion

We have previously described in detail the NEMD techniques used to simulate planar Poiseuille flow [4] and here only summarize the important points. The geometry of the system is shown in Fig. 1, which describes a fluid under planar Poiseuille flow through a narrow channel. We note here that the simulation geometry is such that the driving pressure head is in the x direction and heat will flow in the y direction. Our fluid consists of 738 atoms bound by 54 wall atoms, which are three atomic layers thick (18 atoms per layer). The interatomic potential function $\phi(r)$ was the Weeks-Chandler-Andersen (WCA) potential [6] $\phi(r)=4(r^{-12}-r^{-6})+1$ for $r<2^{1/6}$ and $\phi(r)=0$ for $r>2^{1/6}$ (we have defined the WCA potential constants σ and ε to be unity for simplicity; we also note that the atomic mass has been set to unity). The wall atoms are fixed in place in an fcc lattice structure by a combination of restoring forces and a constraint mechanism, which ensures that the center of mass of the walls remains constant while allowing individual wall atoms the freedom to vibrate about their lattice sites. The simulation cell is periodic in three dimensions to ensure that the overall symmetry and density of the system are preserved. There is only one three atom thick wall per simulation cell. The second wall is simply the periodic image of the first wall. This periodicity also ensures that the total density of the system remains constant.

The equations of motion for the wall particles are

$$\dot{\mathbf{r}}_i = \frac{\mathbf{p}_i}{m} ,$$
$$\dot{\mathbf{p}}_i = -K(\mathbf{r}_i - \mathbf{r}_{ei}) + \sum_{j=1}^{N} \mathbf{F}_{ij} - \alpha \mathbf{p}_i - \mathbf{j}\lambda_{L_j}, \quad i \in L_i , \tag{24}$$

where λ_{L_j} is the layer multiplier and α the thermostat multiplier defined by [4]

$$\lambda_{L_j} = \frac{\mathbf{j}}{n_w} \cdot \sum_{i \in L_j}^{N_w} \left[-K(\mathbf{r}_i - \mathbf{r}_{ei}) + \sum_{k=1}^{N} \mathbf{F}_{ik} \right]$$
$$\text{where } \sum_{L_j=1}^{3} \sum_{i \in L_j}^{N_w} 1 = 3N_w ,$$
$$\alpha = \sum_{i \in L}^{3N_w} \left\{ \left[-K(\mathbf{r}_i - \mathbf{r}_{ei}) + \sum_{j=1}^{N} \mathbf{F}_{ij} - \mathbf{j}\lambda_{L_i} \right] \cdot \mathbf{p}_i \right\} \Big/ \sum_{i \in L}^{3N_w} \mathbf{p}_i^2 . \tag{25}$$

Here N_w is the number of atoms per wall layer and K is the harmonic spring constant. Since there is no streaming motion of the wall particles in any direction, there is no difficulty in distinguishing between laboratory and peculiar momenta for the wall particles, as they are identical.

The fluid particles obey Newton's equations of motion

$$\dot{\mathbf{r}}_i = \frac{\mathbf{p}_i}{m}, \quad \dot{\mathbf{p}}_i = \sum_{j=1}^{N} \mathbf{F}_{ij} + \mathbf{i}F_e , \tag{26}$$

where $\mathbf{F}_{ij}$ is the total WCA force on atom i due to both fluid-fluid and fluid-wall interatomic interactions and $\mathbf{i}F_e$ is the external driving force [4]. It is understood that $\mathbf{p}_i$ is the *laboratory* momentum of particle i (i.e., the sum of the peculiar and streaming components).

B. General simulation considerations

The simulations were conducted using a fifth-order Gear predictor-corrector scheme with an integration timestep of $\tau = 0.001$. The fluid atoms were initially arranged in an fcc structure and the system was allowed to reach steady-state before data were taken. Simulations were carried out at a fluid density of $\bar{n} = N/V = 0.844$.

We denote the unit cell dimensions as, L_x, L_y, L_z, which are given as 4.2238,52.3810,4.2238, respectively. It is important to note that L_y includes the fluid and wall particles (see Fig. 1). For simplicity we make the $y=0$ plane midway between the walls. We note that it is not clear how to determine the *average* density of a fluid because there is no unambiguous definition of the total volume that is accessible to the fluid. This issue has been addressed previously [4] and we comment here that an effective pore width was found to be $l_y = 49.0$.

The simulations were carried out with $F_e = 0.01$ and an optimal wall force constant of $K = 57.15$ [7,8] and were run at a constant wall temperature of 0.722 and wall density of 0.844. Once steady state was achieved, five runs of 90 000 time steps each were undertaken and averages taken of the quantities of interest. In Ref. [4] it was shown that a second-order symmetric polynomial provided a good representation of the streaming velocity of the fluid in the zero flow rate limit and we have once again used such a fit.

The heat flux calculated by MOP, described in Sec. II A, may be compared with those calculated from the Irving-Kirkwood real space expression (1) with $O_{ij} = 1$, (i.e., IK1). We note that IK1 involves summations over a volume V. To find the heat flux as a function of y we thus need to divide the fluid region into bins, each of which has a volume $V_{\mathrm{bin}} = L_x L_z \Delta y$, where L_x and L_z are the lengths of the simulation box in the x and the z directions, respectively, and Δy is the width in the y direction of each bin. The IK1 heat flux, as a function of y, measured in each bin will then be

$$J_{qy}^{\mathrm{bin}}(y,t) = \frac{1}{V_{\mathrm{bin}}} \left[\sum_{i \in \mathrm{bin}} [\mathbf{v}_i - \mathbf{u}(y)] U_i - \frac{1}{2} \sum_{\substack{i,j \\ i \in \mathrm{bin}}} \mathbf{r}_{ij} [\mathbf{v}_i - \mathbf{u}(y)] \cdot \mathbf{F}_{ij} \right]_y , \tag{27}$$

where now the sum over i includes only atoms that are contained within the bin and the sum over j includes all possible atoms within or outside the bin.

We can also calculate other quantities as a function of y by summing them over bins, such as the velocity, the temperature, and the density. In all our simulations we used 251 bins, such that $\Delta y = 0.2$.

The internal energy U_i of atom i at the time of intersection with any plane was calculated by an interpolation scheme in which a polynomial is fit to the energy values of the previous four time steps. Since the energy varied slowly over such short times, only a least-squares cubic polynomial interpolating function was required. The time of intersection with any particular plane was calculated by the standard Newton-Raphson interpolation. The code used to calculate MOP heat flux vector was checked by calculating $\mathbf{J}_q$ in a system with a homogeneous heat flux generated by the Evans heat flow algorithm and gave excellent agreement with the zero wave vector Irving-Kirkwood heat flux vector.

$P_{xy}(y)$, used for calculating the mesoscopic heat flux vector, was calculated by the IMC method, as this has been shown to have better statistics than MOP [4].

IV. RESULTS

Figure 2 displays a plot of $J_{qy}(y)$ across the entire pore width, calculated by both MOP and IK1. Similar to the case of the pressure tensor calculation [4], MOP is shown

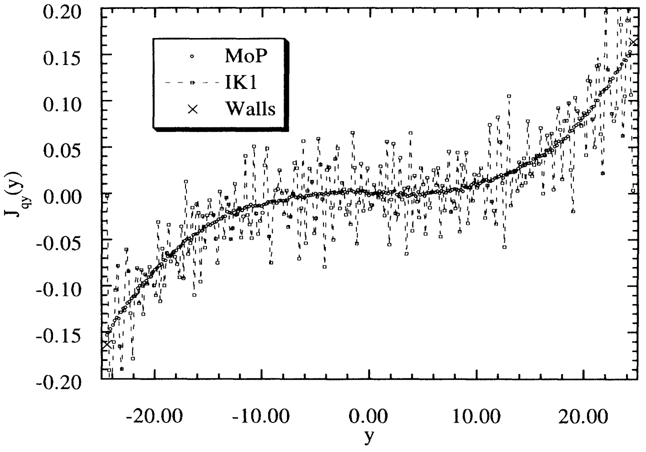

FIG. 2. $\mathbf{J}_{qy}(y)$ calculated by MOP and IK1. Also shown is the value of the heat flux at the walls.

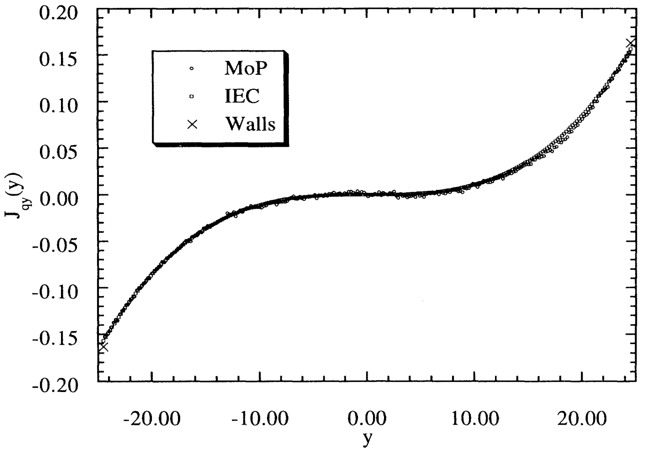

FIG. 3. Comparison of $\mathbf{J}_{qy}(y)$ calculated by MOP and IEC.

to be a much more accurate method. Indeed MOP implicitly includes within it the full expansion of all the O_{ij} terms, so it is not surprising that this should be the case.

Also shown in Fig. 2 is $J_{qy}(y)$ measured at the walls. It has been shown [2] that Gaussian thermostats remove heat from a system at the rate

$$\dot{Q}(t)=\alpha(t)\sum_{i=1}^{N}\frac{\mathbf{p}_i^2}{m_i}\ , \qquad (28)$$

where N is the number of particles in the system. Thus the heat flux at the walls can be determined by calculating the heat extracted from the walls by the thermostat, i.e.,

$$\langle J_{qy}(y_{\rm wall})\rangle=\frac{1}{A}\langle K_w\alpha\rangle\ , \qquad (29)$$

where K_w is the kinetic energy of the wall atoms and the angular brackets indicate a time average. We note here that the y position of the fluid-wall interface $y_{\rm wall}$ is, like the effective length l_y of the pore (described in Sec. III B), an ambiguous quantity to define. For consistency, we have thus defined it to be $y_{\rm wall}=\pm l_y/2$. Once again we see good agreement between MOP and $J_{qy}(y)$ measured at the walls.

Figure 3 compares $J_{qy}(y)$ across the pore calculated by the MOP and IEC techniques. Both methods are seen to be in excellent agreement with each other. The IEC method in fact displays superior statistics, seen more clearly in Fig. 4, which is a plot of the standard deviations in $J_{qy}(y)$ for both methods. We note here that the IEC calculation requires a knowledge of the stress and that we have used the IMC method to calculate this quantity. In Ref. [4] it was shown that the IMC technique for calculating $P_{xy}(y)$ is more accurate than the corresponding MOP method. It was also shown that the IMC calculation involved a numerical integration of the density profile. It is because this density profile is so stable, and thus has very good statistics, that the IEC method of calculating $J_{qy}(y)$ is superior to MOP.

Finally, we make a comment on the use of either peculiar or plane peculiar velocities in the calculation of $J_{qy}(y)$ via MOP, as shown in Fig. 5. The quadratic streaming velocity of the fluid in our system does not have sufficient curvature to generate any difference in $J_{qy}(y)$ calculated by use of either peculiar or plane peculiar velocities, even though the use of the latter is formally correct. However, this agreement should be regarded as a fortuitous consequence of the relatively gentle curvature in our velocity profile and we emphasize again that higher curvature profiles (e.g., a profile generated from a high spatial frequency sinusoidal external field) should be expected to give incorrect values of the heat flux if the plane peculiar velocities are not used.

V. CONCLUSIONS

We have extended the method of planes derivation that we first employed to calculate the exact pressure tensor in inhomogeneous systems, to the formulation of the heat flux vector. The MOP expression was then applied to the special case of planar Poiseuille flow and was found to be much more reliable than the corresponding IK1 approxi-

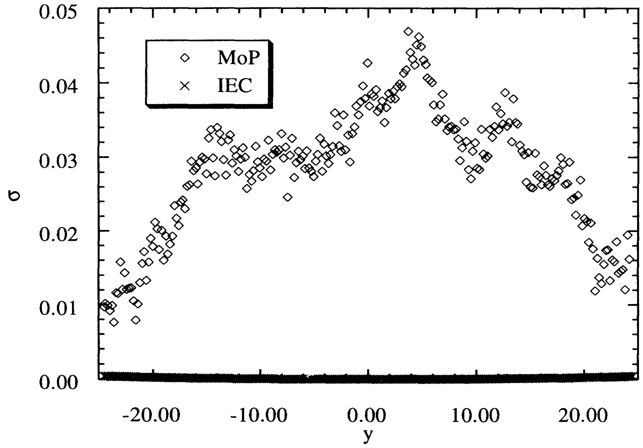

FIG. 4. Standard deviations in $\mathbf{J}_{qy}(y)$ for MOP and IEC.

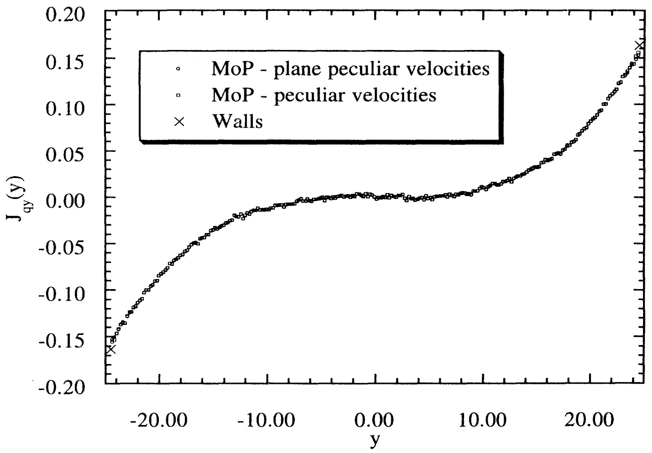

FIG. 5. Comparison of the MOP calculations of $\mathbf{J}_{qy}(y)$ using the correct plane peculiar velocities and the formally incorrect peculiar velocities.

mation. It avoids the cumbersome Taylor series expansion of δ function differences that would be required for the full Irving-Kirkwood derivation and, in fact, implicitly includes an exact infinite-order summation of the Irving-Kirkwood O_{ij} operator expansion.

In addition, we have, for the special case of planar Poiseuille flow, derived another equation for $J_{qy}(y)$, based upon a mesoscopic integration of the energy continuity equation (IEC). Both the MOP and the IEC methods are shown to have excellent numerical agreement with each other, with the IEC technique having superior statistics, though we note that the use of the latter is limited in that it is valid here only for the particular case of planar Poiseuille flow. The MOP technique is, however, more general and for this reason is potentially the more useful of the two methods.

We introduce the curious concept of a "plane peculiar velocity" χ, which must be used instead of the usual peculiar velocity in the calculation of $J_{qy}(y)$ by MOP. We note that for streaming velocity profiles that are gentle in curvature there is no noticeable difference if the heat flux is calculated by using either peculiar or plane peculiar velocities, even though the latter is the formally correct velocity to use. However, if the curvature of the streaming velocity profile is significant, we would expect errors to be introduced into the calculation of the heat flux if peculiar velocities are used.

Finally, we point out that the techniques developed here to calculate $J_{qy}(y)$ now give us a means by which to calculate the spatially dependent thermal conductivity of a fluid in a nonhomogenous system, in the same way that the MOP and IMC methods of calculating the P_{xy} component of the pressure tensor enabled us to calculate the spatial dependency of the viscosity of such a fluid. These calculations are currently being performed.

ACKNOWLEDGMENTS

We would like to thank the Australian National University Supercomputer Facility for a substantial allocation of computer time and P.J.D. thanks Dr. Gary Morriss for helpful discussions regarding the resummation of Eq. (A9).

APPENDIX

The standard Irving-Kirkwood derivation of the ensemble-averaged heat flux vector is well known, but it is rather complicated due to the necessity of introducing a series expansion for the difference between two δ functions. We show here that it is simpler to carry out the first part of the derivation in **k** space and then inverse transform to obtain the standard Irving-Kirkwood result. The Irving-Kirkwood result is simply the ensemble average of our expression.

We begin our derivation of the expression for the instantaneous heat flux vector by Fourier transforming the energy continuity equation [Eq. (4)] and solving for the term involving $\mathbf{J}_q$. The right-hand side then consists of three terms: the first is the partial derivative with respect to time of the internal energy density, which is expressed in terms of microscopic quantities as

$$\begin{aligned}\frac{\partial}{\partial t}\rho e(\mathbf{k},t) &= i\mathbf{k}\cdot\sum_i \mathbf{v}_i e_i e^{i\mathbf{k}\cdot\mathbf{r}_i}+\tfrac{1}{2}\sum_i\sum_j \mathbf{v}_i\cdot\mathbf{F}_{ij}(e^{i\mathbf{k}\cdot\mathbf{r}_i}-e^{i\mathbf{k}\cdot r_j})\\ &= i\mathbf{k}\cdot\sum_i \mathbf{v}_i e_i e^{i\mathbf{k}\cdot r_i}\\ &\quad -i\mathbf{k}\cdot\tfrac{1}{2}\sum_i\sum_j \mathbf{r}_{ij}\mathbf{F}_{ij}\cdot\mathbf{v}_i g(k,t)e^{i\mathbf{k}\cdot\mathbf{r}_i}\ ,\end{aligned} \tag{A1}$$

where

$$g(k,t)=\frac{(e^{i\mathbf{k}\cdot\mathbf{r}_{ij}}-1)}{i\mathbf{k}\cdot\mathbf{r}_{ij}}\ ; \tag{A2}$$

the second term has already been given in Eq. (7); and the third term, which is the Fourier transform of the scalar product of the pressure tensor with the streaming velocity, will be left in its original form for the moment. Our equation for $\mathbf{J}_q$ is then

$$\begin{aligned}\mathbf{J}_q(\mathbf{k},t) &= \sum_i(\mathbf{v}_i-\mathbf{u}_i)e_i e^{i\mathbf{k}\cdot\mathbf{r}_i}\\ &\quad -\tfrac{1}{2}\sum_i\sum_j \mathbf{r}_{ij}\mathbf{F}_{ij}\cdot\mathbf{v}_i g(k,t)e^{i\mathbf{k}\cdot\mathbf{r}_i}-\mathcal{F}\{\mathbf{P}\cdot\mathbf{u}\}\ .\end{aligned} \tag{A3}$$

The next step is more easily performed in **r** space, so we inverse transform and use the **r**-space microscopic expression for $\mathbf{P}\cdot\mathbf{u}$

$$\begin{aligned}\mathbf{P}(\mathbf{r},t)\cdot\mathbf{u}(\mathbf{r},t) &= \sum_i m_i(\mathbf{v}_i-\mathbf{u})(\mathbf{v}_i-\mathbf{u})\cdot\mathbf{u}\delta(\mathbf{r}-\mathbf{r}_i)\\ &\quad -\tfrac{1}{2}\sum_i\sum_j \mathbf{r}_{ij}\mathbf{F}_{ij}\cdot\mathbf{u}O_{ij}\delta(\mathbf{r}-\mathbf{r}_i)\end{aligned} \tag{A4}$$

and the relationship

$$g(\mathbf{k},t)e^{i\mathbf{k}\cdot\mathbf{r}_i}=\mathcal{F}\{O_{ij}\delta(\mathbf{r}-\mathbf{r}_i)\} \tag{A5}$$

to obtain

$$\begin{aligned}\mathbf{J}_q(\mathbf{r},t) &= \sum_i(\mathbf{v}_i-\mathbf{u})U_t\delta(\mathbf{r}-\mathbf{r}_i)\\ &\quad -\tfrac{1}{2}\sum_i\sum_j \mathbf{r}_{ij}\mathbf{F}_{ij}\cdot(\mathbf{v}_i-\mathbf{u})O_{ij}\delta(\mathbf{r}-\mathbf{r}_i)\ .\end{aligned} \tag{A6}$$

This is the instantaneous form of the Irving-Kirkwood expression for the heat flux vector. The **k**-space version of this equation is now obtained directly by Fourier transformation. Because **u** is a function of **r**, the Fourier transform of this equation must be performed with the aid of the identity

$$\int_{-\infty}^{\infty} dx\, f(x)\frac{\partial^n}{\partial x^n}\delta(x-a)=(-1)^n f^n(a)\ , \tag{A7}$$

giving

$$\begin{aligned}\mathcal{F}\{\mathbf{u}O_{ij}\delta(\mathbf{r}-\mathbf{r}_i)\}&=\int_{-\infty}^{\infty} d\mathbf{r}\, e^{i\mathbf{k}\cdot\mathbf{r}}\mathbf{u}O_{ij}\delta(\mathbf{r}-\mathbf{r}_i)\\ &=\sum_{n=0}^{\infty}\frac{(-1)^n}{(n+1)!}\int_{-\infty}^{\infty} d\mathbf{r}\, e^{i\mathbf{k}\cdot\mathbf{r}}\mathbf{u}\left[\mathbf{r}_{ij}\cdot\frac{\partial}{\partial\mathbf{r}}\right]^n\delta(\mathbf{r}-\mathbf{r}_i)=\sum_{n=0}^{\infty}\frac{1}{(n+1)!}\int_{-\infty}^{\infty} d\mathbf{r}\,\delta(\mathbf{r}-\mathbf{r}_i)\left[\mathbf{r}_{ij}\cdot\frac{\partial}{\partial\mathbf{r}}\right]^n(e^{i\mathbf{k}\cdot\mathbf{r}}\mathbf{u})\\ &=\sum_{n=0}^{\infty}\frac{1}{(n+1)!}\left[\mathbf{r}_{ij}\cdot\frac{\partial}{\partial\mathbf{r}}\right]^n(e^{i\mathbf{k}\cdot\mathbf{r}}\mathbf{u})\Bigg|_{\mathbf{r}=\mathbf{r}_i}\ .\end{aligned}\tag{A8}$$

The final result is then

$$\mathbf{J}_q(\mathbf{k},t)=\sum_i(\mathbf{v}_i-\mathbf{u}_i)U_i e^{i\mathbf{k}\cdot\mathbf{r}_i}-\tfrac{1}{2}\sum_i\sum_j\mathbf{r}_{ij}\mathbf{F}_{ij}\cdot\sum_{n=0}^{\infty}\frac{1}{(n+1)!}\left[\mathbf{r}_{ij}\cdot\frac{\partial}{\partial\mathbf{r}}\right]^n[e^{i\mathbf{k}\cdot\mathbf{r}}(\mathbf{v}_i-\mathbf{u})]\Bigg|_{\mathbf{r}=\mathbf{r}_i}\ , \tag{A9}$$

where we have also used the relationship

$$g(\mathbf{k},t)e^{i\mathbf{k}\cdot\mathbf{r}_i}=\sum_{n=0}^{\infty}\frac{1}{(n+1)!}\left[\mathbf{r}_{ij}\cdot\frac{\partial}{\partial\mathbf{r}}\right]^n[e^{i\mathbf{k}\cdot\mathbf{r}}]\Bigg|_{\mathbf{r}=\mathbf{r}_i}\ . \tag{A10}$$

Explicit differentiation and resummation of terms in Eq. (A9) results in the expression

$$\mathbf{J}_q(\mathbf{k},t)=\sum_i(\mathbf{v}_i-\mathbf{u}_i)U_i e^{i\mathbf{k}\cdot\mathbf{r}_i}-\tfrac{1}{2}\sum_i\sum_j\mathbf{r}_{ij}\mathbf{F}_{ij}\cdot e^{i\mathbf{k}\cdot\mathbf{r}_i}\exp\left[-i\frac{\partial}{\partial\mathbf{k}}\cdot\frac{\partial}{\partial\mathbf{r}}\right]\{g(\mathbf{k},t)[\mathbf{v}_i-\mathbf{u}(\mathbf{r},t)]\}\big|_{\mathbf{r}=\mathbf{r}_i}\ . \tag{A11}$$

It is easily verified that this equation agrees with Eq. (A9), in both the $\mathbf{k}=0$ and $\mathbf{u}=0$ limits. Equation (A11) is useful when the velocity profile can be expressed as a polynomial of known order.

[1] J. H. Irving and J. G. Kirkwood, J. Chem. Phys. **18**, 817 (1950).
[2] D. J. Evans and G. P. Morriss, *Statistical Mechanics of Nonequilibrium Liquids* (Academic, London, 1990).
[3] D. MacGowan and D. J. Evans, Phys. Lett. A **117**, 414 (1986).
[4] B. D. Todd, D. J. Evans, and P. J. Daivis (unpublished).
[5] P. J. Daivis and D. J. Evans, Mol. Phys. **81**, 1289 (1994).
[6] J. D. Weeks, D. Chandler, and H. C. Andersen, J. Chem. Phys. **54**, 5237 (1971).
[7] S. Y. Liem, D. Brown, and J. H. R. Clarke, Phys. Rev. A **45**, 3706 (1992).
[8] S. Murad, P. Ravi, and J. G. Powles, Phys. Rev. E **48**, 4110 (1993).